This is a repository copy of *Disorder-order morphologies in drop-tube processed Ni3Ge: Dendritic and seaweed growth*.

White Rose Research Online URL for this paper:
http://eprints.whiterose.ac.uk/107439/

Version: Accepted Version

Article:

Accepted Manuscript

Disorder-order morphologies in drop-tube processed Ni$_3$Ge: Dendritic and seaweed growth

Nafisul Haque, Robert F. Cochrane, Andrew M. Mullis

Please cite this article as: N. Haque, R.F. Cochrane, A.M. Mullis, Disorder-order morphologies in drop-tube processed Ni$_3$Ge: Dendritic and seaweed growth, *Journal of Alloys and Compounds* (2016), doi: 10.1016/j.jallcom.2016.11.080.

Disorder-order morphologies in drop-tube processed Ni₃Ge: Dendritic and Seaweed Growth

Nafisul Haque[1, a], Robert F. Cochrane[1], Andrew M. Mullis[1]

[1]Institute for Material Research, University of Leeds, Leeds LS2-9JT, UK

[a]Corresponding author: pmnh@leeds.ac.uk

Keywords: Intermetallic; rapid solidification; phase transitions; dendrites; seaweed structure.

Abstract

The single phase intermetallic β-Ni₃Ge has been subject to rapid solidification via drop-tube processing. Droplets spanning the size range $212 - 38$ μm, with corresponding cooling rates of $5800 - 54500$ K s⁻¹, have been subject to microstructural investigation using SEM. Three dominant solidification morphologies have been identified with increasing cooling rate, namely; (i) well-defined dendrites with orthogonal side-branching, (ii) dendrites with non-orthogonal side-branching and (iii) dendritic seaweed. Selected area diffraction analysis in the TEM reveals that both types of dendrites are the disordered form of β-Ni₃Ge in a matrix of the ordered, L1₂, form. However, the diffraction pattern from the dendritic seaweed cannot be mapped onto a cubic structure, indicating a change in the underlying crystallography coincident with the transition to the seaweed structure.

Introduction

During near-equilibrium solidification, metals typically crystallise into morphologies displaying a strong directionality imposed by the 'easy' growth directions in the underlying crystalline anisotropy. More specifically, these are directions of minimum capillary stiffness whereby the melting temperature is most highly depressed by the Gibbs-Thomson effect. Typically, this results in the growth of structure such as dendrites, which for metals with an underlying cubic symmetry, will display well developed side-arms orthogonal to the primary trunk. However, with increasing departure from equilibrium a number of changes may be manifest in these solidification structures, including a switch in the growth direction away from these easy directions or a more general loss of

directionality in the solidification morphology [1]. The first of these typically results in a switch from the equilibrium <100> growth direction, to growth along either the <110> or <111> directions, with the <100> to <110> transition having been observed directly in the transparent analogue casting system $NH_4Cl - H_2O$ [2]. In such a transition the primary solidification morphology remains dendritic, but the transition is evidenced by a switch to side-branches which are no longer orthogonal to the primary trunk [1, 3]. This sometimes occurs coincident with a break in the gradient of velocity-undercooling curve [4]. Further evidence can be provided by X-ray or EBSD pole-figure plots [4] or selected area diffraction patterns from the TEM. Such a switch in the growth direction usually occurs abruptly at a well-defined undercooling and is normally attributed to a competition between differently directed kinetic and surface energy anisotropies. The same mechanism is also thought to be responsible for the more general loss in directionality during rapid solidification, possibly as competing anisotropies cancel out [5]. This results in solidification morphologies such as doublons and dendritic seaweed. Such structures have been observed in the transparent analogue casting system $CBr_4 - C_2Cl_6$ [6], polymers [7] and metals [8, 9]. Typically this transition is more diffuse than the well-defined switch in growth direction, occurring gradually over a range of undercoolings or with the transition being prefaced by a change in growth direction [1]. Indeed, it has been demonstrated that in certain alloys a continuous range of growth directions can be accessed prior to a transition to seaweed type growth [10].

Within the broad class of metallic materials, it is not only solid-solution alloys that have been shown to display a dendritic to seaweed growth transition, but also intermetallic compounds. Specifically, Assadi *et al.* [11] have shown that the congruently melting intermetallic NiAl may undergo a dendritic to seaweed transition at an undercooling around 250-265 K when close to the congruent composition. Close to equilibrium NiAl solidifies to the ordered cubic B2 crystal structure direct from the melt. Assadi *et al.* propose that it is disorder trapping during rapid solidification and the loss of long range chemical order within the intermetallic that drives the dendritic to seaweed transition. Disorder trapping may be considered analogous to the more familiar process of solute trapping. However, rather than a non-equilibrium solute distribution occurring at the solid-liquid interface, increasing

solidification velocity sees progressively higher levels of chemical disorder trapped in the structure [12]. They argue that loss of long range order at the fast growing dendrite tip leads to an extreme depression of the melting temperature which can 'mask' the interfacial stiffness. Coupled with increased orientational disorder, which increases the free energy of the solid, this makes the system behave in a low anisotropy manner.

If this model is indeed correct, other congruently melting intermetallics are also likely to show a dendritic to seaweed transition under rapid solidification conditions. The only other condition is that during equilibrium solidification the compound should order at the liquidus temperature, such that disorder trapping is possible. One such intermetallic that satisfies both conditions is β-Ni$_3$Ge. This system has previously been studied by Ahmed *et al*. [13] who, using a flux undercooling technique, observed a maximum undercooling of 362 K, wherein the corresponding growth velocity was measured at 3.55 m s^{-1}. In common with other researchers who have determined the velocity-undercooling curves for intermetallic compounds passing through the order-disorder transformation, [13] observed a discontinuous break in the curve at the onset of fully disordered growth. This condition was observed for β-Ni$_3$Ge at an undercooling of 168 K and at a critical growth velocity, V_C, of 0.22 m s^{-1}. This compares with $V_C = 0.75$ m s^{-1} in Fe-18 at. % Ge [14] and $V_C = 3.8$ m s^{-1} in CoSi [15]. Microstructural analysis of the β-Ni$_3$Ge system [13] revealed a transition from a coarse grained structure during ordered growth to a much finer grained structure once disordered growth was achieved. However, due to the low cooling rate achieved during flux undercooling (~10 K s^{-1}), the original solidification morphology is likely to have been highly modified during post-recalescence cooling.

In this paper we use drop-tube processing to explore the rapid solidification behaviour of β-Ni$_3$Ge. Unlike flux undercooling techniques, drop-tube processing provides access to high post-recalescence cooling rates, wherein inherently unstable structures such as dendritic seaweed may be retained. The objective of the work is to explore whether the dendritic to seaweed transition observed in NiAl can be replicated in any other congruently melting intermetallic and to throw further light of the formation mechanism.

Experimental Methods

According to the phase diagram of Nash and Nash [16], β-Ni₃Ge is a congruently melting compound with a melting point of 1405 K. It has a homogeneity range of 22.5 to 25 at. % Ge and crystallizes to the ordered fcc L12 structure. Ni3Ge also occurs as γ-phase, a stoichiometric intermetallic with composition 25.6 at.% Ge which forms via the peritectic reaction $L + \beta \rightarrow \gamma$ at 1391 K. This subsequently undergoes a further peritectic decomposition to δ-Ni5Ge2 at 1380 K [17]. However, as γ-Ni3Ge is typically only observed after extend (1-24 h) ageing at elevated temperatures [18] we think its occurrence unlikely during rapid solidification processing.

For the drop-tube experiments reported here, elemental Ni and Ge were obtained from Alfa Aesar with purity of 99.99 % and 99.999%, metals basis, respectively. The alloy, of composition Ni-25 at. % Ge, was produced by arc-melting the elemental constituents together under a protective argon atmosphere, with the melting process being repeated 8 times to ensure uniform mixing of the final alloy. Following arc-melting the phase composition of the alloy ingot was checked using a PANalytical Xpert Pro X-ray diffractometer to ensure that single phase β-Ni₃Ge had been obtained.

The single-phase β-Ni₃Ge ingot was then subject to rapid solidification by drop-tube processing. The alloy sample, of approximately 9.5 g mass, was loaded into an alumina crucible with three 300 µm laser drilled holes in the base. Induction heating of a graphite subsector was used to melt the sample. Temperature determination was by means of an R-type thermocouple which sits inside the melt crucible, just above the level of the melt. When the temperature in the crucible attained 1480 K (75 K superheat) the melt was ejected by pressurising the crucible with ~ 400 kPa of N₂ gas. The resulting spray of particles solidify in-flight whilst falling the 6.5 m length of the tube, which is filled to 50 kPa with dry, oxygen free N₂ gas. Further details of the drop-tube method are given in [19].

Following retrieval of the sample from the base of the drop-tube the powders were sieved into standard size fractions, with the size fractions, 212 - 150 µm, 106 - 75 µm and 53 – 38 µm being selected for analysis here. Using the method given by [19] the mean post-recalescence cooling rate for these three size fractions is estimated as 5800 K s⁻¹, 30000 K s⁻¹ and 54500 K s⁻¹ respectively.

The selected size fractions were subject to XRD analysis to ensure they remained single-phase and were then mounted in transopic resin and prepared for microstructural analysis. This involved grinding with SiC grinding media and then polishing with progressively finer grades of diamond paste, finishing with a 1 µm grade. β-Ni$_3$Ge was found to be highly resistant to most chemical etchants normally used in metallography. The etchant used was the aggressive mix consisting equal parts of undiluted HF, HCl and HNO3. A Carl Zeiss EVO MA15 scanning electron microscopy (SEM) was used to image the microstructure of the droplets revealed by etching while an Oxford Instrument X-Max Energy-Dispersive X-Ray (EDX) detector was used to check the chemical homogeneity of the samples. Selected area diffraction analysis and bright-field imaging was performed using a FEI Tecnai TF20 Transmission Electron Microscope (TEM), with samples, of approximately 10 µm × 7 µm and between 55-70 nm in thickness, being cut from the mounted and polished specimens using a FEI Nova 200 Nanolab focused ion beam (FIB).

Results & Discussion

The starting material for the drop-tube experiments was single phase β-Ni3Ge, this being confirmed by XRD analysis on the polished surface of the arc-melted ingot. It can be seen from Figure 1(a) that all the XRD peaks may be reliably indexed to the β-Ni3Ge phase using the ICCD reference pattern 04-004-3112. When similar material was deeply undercooled by Ahmad et al., using a melt fluxing technique, the resultant material remained single phase β-Ni3Ge [20] for all undercoolings studied. XRD analysis reveals that the same is true during rapid cooling via drop-tube processing, with the drop-tube powders 850 µm - 150 µm [21] and 150 µm - 38 µm displaying peaks that can unambiguously be associated with the Ni3Ge reference pattern.

Figure 2(a) shows an SEM micrograph of a polished and etched sample from the (a) 212 - 150 µm sieve fraction. The dominant morphology is that of clearly defined and well delineated dendrites with clear, orthogonal side-branching. The contrast between the dendrite and the surrounding matrix material is unusual for a fully crystalline material, with this type of contrast being more usual in a partially crystalline-partially amorphous material. Moreover, this contrast is not the result of

compositional differences between the dendrite and the surrounding matrix due to solute partitioning during solidification. The absence of solute partitioning is demonstrated in Figure 2(b) which shows an EDX line scan perpendicular to a primary dendrite truck as revealed by etching. From this it is clear that, to within the experimental error associated with the technique, there is no variation in composition between the structures revealed by etching (see Figure 2) and the surrounding featureless matrix.
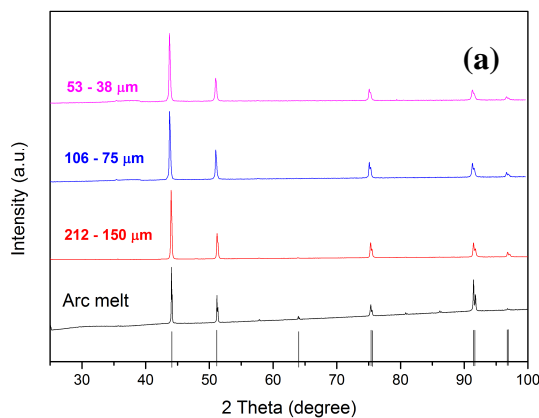

Figure 1: (a) X-Ray diffraction analysis of an arc melted sample prior to drop-tube process (black) and three drop-tube processed powders of varying sizes. Vertical black lines indicate peak positions for the β-Ni3Ge reference pattern.

The origin of the contrast, as elucidated by selected area diffraction techniques in the TEM, will be discussed shortly. For the time being however we note that the TEM analysis indicates that the material is fully crystalline. With a reduction in the particle size to 106 - 75 μm (Figure 3) the solidification morphology remains dendritic but the dendrites begin to show typical rapid solidification traits, in particular side-branches that are no longer orthogonal to the main trunk and irregular splitting of arms as if taking on a doublon type character. In particular, for the dendrite towards the top of the droplet as pictured, sketched in red in Figure 3(b), the angle between the primary trunk and the secondary arms varies between 45° at the left of the droplet (as viewed) to 63° at its right-hand end (mean 51.2°). Over its length the growth direction of the primary trunk changes by some 18°. Conversely, for the dendrite close to the centre of the droplet, sketched in blue in Figure 3(b), the angle between the primary trunk and the longer part of the secondary arms (also shown in

blue) is close to 45° along the whole length of the dendrite, while for the smaller branches, emanating near the root of each secondary arm and shown in green, the angle is close to 30°. The transition from orthogonal to non-orthogonal side-branching with increasing undercooling in a cubic system is indicative of a change in the primary growth direction away from the [100] direction that would be expected at equilibrium and has been observed in a number of systems previously [3]. Such a change has itself previously been observed as precursor to the change from a dendritic to dendritic seaweed transition [1].

We also note the very distinct curvature of this dendrite, with a change in growth direction of close to 30°. While such curved dendrites have previously been noted as a consequence of flow during rapid solidification [22], the droplet size here is likely to be too small for this to be a plausible mechanism for the observed curvature, which may instead be indicative of a more general decrease in directionality within the microstructure.
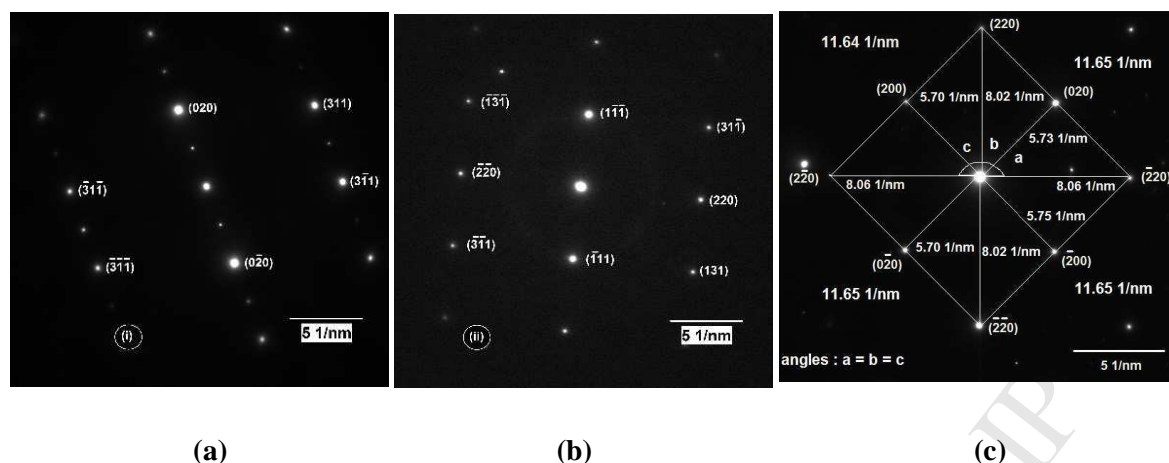
Figures 4(a & b) show two selected area diffraction patterns obtained from the microstructure shown in Figure 2(a). Figure 4(a) is taken from the featureless matrix material well away from the dendrite and is consistent with the expected ordered $L1_2$ crystal structure for β-Ni_3Ge. In contrast Figure 4(b) is taken from the centre of the dendrite. This also displays a cubic structure with the same lattice spacing as the matrix material. However, the superlattice spots indicative of an ordered structure are absent, indicating that the dendrite is the disorderd form of the material, this being a simple A1 fcc random solid solution. These observations may be interpreted by postulating that the dendrites are the rapid solidification morphology and grew as the disordered form of β-Ni_3Ge due to extensive disorder trapping. The matrix material would then have formed post-recalescence, growing as the ordered form of β-Ni_3Ge due to the much lower growth rate. The clear contrast between dendrite and matrix seen in Figure 2(a) is, we believe, a consequence of preferential etching of the disordered phase, with the ordered material being more resistant to the etch.
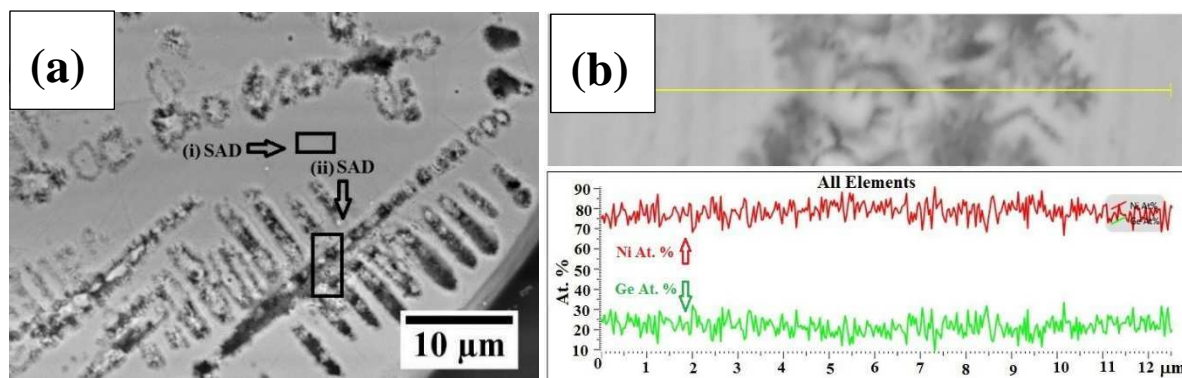
Figure 2: (a) SEM micrograph of HF etched β-Ni₃Ge drop-tube particle from the 212 – 150 µm size fraction showing dendritic structures in a featureless matrix and (b) EDX line scan across a dendrite trunk showing that the contrast revealed by etching is not the result of solute partitioning.
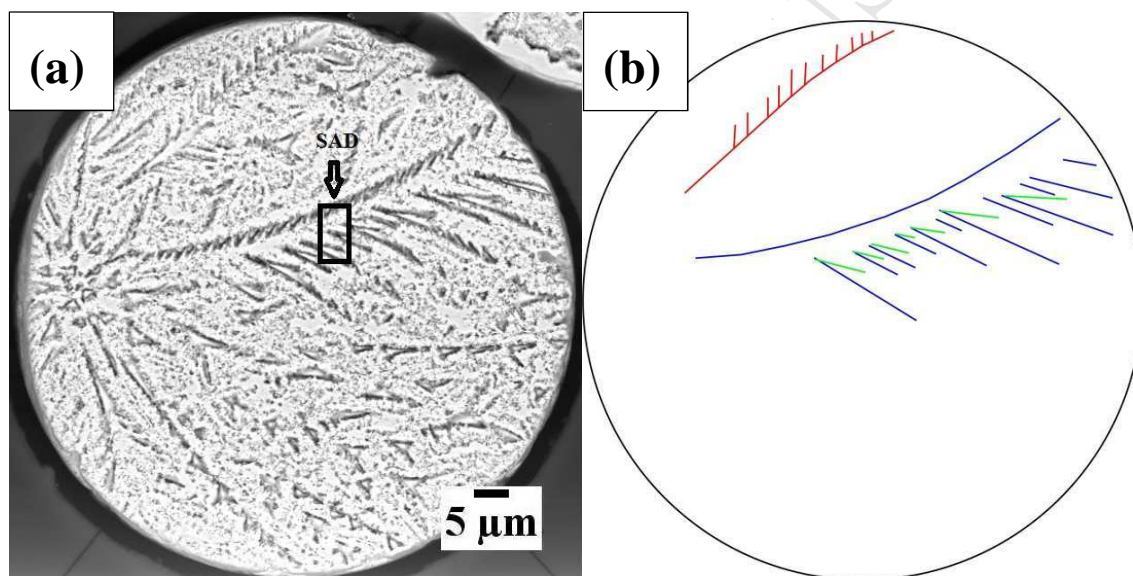
Figure 3: (a) SEM micrographs of HF etched β-Ni₃Ge drop-tube particles from the 106 – 75 µm size fraction showing dendritic structure with non-orthogonal side-branching and (b) sketch of same highlighting two bent dendrites with non-orthogonal side-branching.

(a)   **(b)**   **(c)**

Figure 4: Selected area diffraction patterns (SAD) from (a) Figure 2a matrix materials well away from the dendrite, (b) Figure 2a inside the dendrite and (c) Figure 3a inside the dendrite.

Figure 4(c) is the selected area diffraction pattern obtained from the dendritic region in Figure 3. Despite the now rather erratic nature of the dendrite morphology, with side-branches at various angles to their respective primary trunks and evidence of tip-splitting, the underlying crystal structure is identical to that found in the larger droplets. As such, the TEM data provides clear evidence that the change in dendrite morphology must arise from a change in the preferred growth direction within the same crystal structure, rather than a change in phase present.

Finally, Figure 5 shows (a) the SEM micrograph and (b) the corresponding TEM selected area diffraction pattern from a droplet in the $53 - 38$ μm sieve fraction. The morphology is now clearly that of a dendritic seaweed, with both multiple tip-splitting and a clear lack of directionality being evident. With regard to Figure 5(b), while we have not been able to unambiguously index the TEM selected area diffraction pattern, it does not conform to the $L1_2$ cubic model. This would appear to indicate that the transition to the seaweed structure is coincident with a change in the underlying crystal structure. This is contrary to the accepted model for seaweed formation which postulates that, as with the change in dendrite growth direction, the underlying crystal structure remains unchanged. Given the lack of evidence for any solid-solution alloy displaying such a change in underlying crystallography coincident with the dendritic to seaweed transition, we are inclined to believe that this phenomenon may be peculiar to intermetallics or possibly even this compound (unfortunately [11] do not report

any crystallographic determination from the seaweed morphology in NiAl). One possible explanation may be that high levels of disorder in the orientational ordering that [11] postulate to be required for seaweed growth results in a severe distortion of the crystal lattice.
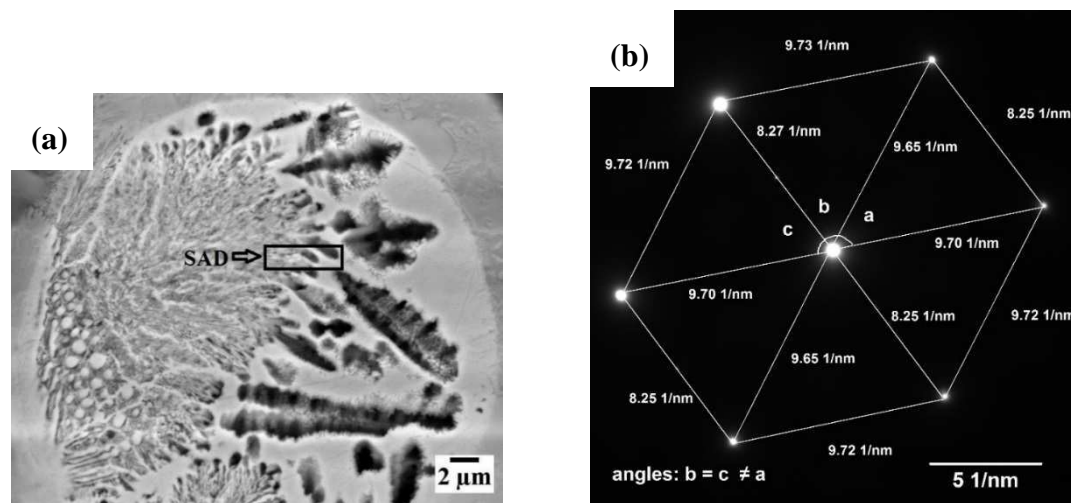
Figure 5: (a) SEM micrograph of an HF etched β-Ni$_3$Ge drop-tube particle from the 53 – 38 μm size fraction showing dendritic structures in a featureless matrix, (b) selected area diffraction patterns from region identified in the SEM micrograph.

Summary & Conclusion

Drop-tube processing has been used to rapidly solidify single phase β-Ni$_3$Ge into droplets spanning the size range 212 – 38 μm. The corresponding range of cooling rates is 5800 - 54500 K s^{-1}. At low cooling rates the solidification morphology consists of dendrites of the disordered phase, which are the rapid solidification morphology, embedded within a matrix of the ordered phase which grew more slowly post-recalescence. With increasing cooling rate the dendrites display non-orthogonal side-branching together with some tip-splitting, although the underlying crystallography, as revealed by selected area diffraction analysis in the TEM, remains the same as at lower cooling rate. At the highest cooling rates studied dendritic growth is replaced by that of dendritic seaweed. This is accompanied by a change in the underlying crystallography, which can no longer be modelled as cubic, although the space group corresponding to the seaweed material remains to be identified. This is, as far as we are aware, the first instance in which a transition from dendritic to seaweed growth

mediated purely by an increase in undercooling, has been observed to be coincident with a change in the underlying crystallography of the material.

Acknowledgements

References

[1] E.G. Castle, A.M. Mullis, R.F. Cochrane, Evidence for an extensive, undercooling-mediated transition in growth orientation, and novel dendritic seaweed microstructures in Cu–8.9 wt.% Ni, Acta Materialia, 66 (2014) 378-387.

[2] Y. Sawada, Transition of growth form from dendrite to aggregate, Physica A, 140 (1986) 134-141.

[3] E.G. Castle, A.M. Mullis, R.F. Cochrane, Mechanism selection for spontaneous grain refinement in undercooled metallic melts, Acta Materialia, 77 (2014) 76-84.

[4] K. Dragnevski, R. Cochrane, A. Mullis, The solidification of undercooled melts via twinned dendritic growth, Metallurgical and Materials Transactions A, 35 (2004) 3211-3220.

[5] A. Mullis, A study of kinetically limited dendritic growth at high undercooling using phase-field techniques, Acta Materialia, 51 (2003) 1959-1969.

[6] S. Akamatsu, G. Faivre, T. Ihle, Symmetry-broken double fingers and seaweed patterns in thin-film directional solidification of a nonfaceted cubic-crystal, Physical Review E, 51 (1995) 4751-4773.

[7] K. Taguchi, H. Miyaji, K. Izumi, A. Hoshino, Y. Miyamoto, R. Kokawa, Growth shape of isotactic polystyrene crystals in thin films, Polymer, 42 (2001) 7443-7447.

[8] K. Dragnevski, R. Cochrane, A. Mullis, Experimental evidence for dendrite tip splitting in deeply undercooled, ultrahigh purity Cu, Physical review letters, 89 (2002) 215502.

[9] A. Mullis, K. Dragnevski, R. Cochrane, The transition from the dendritic to the seaweed growth morphology during the solidification of deeply undercooled metallic melts, Materials Science and Engineering: A, 375 (2004) 157-162.

[10] T. Haxhimali, A. Karma, F. Gonzales, M. Rappaz, Orientation selection in dendritic evolution, Nature Materials, 5 (2006) 660-664.

[11] H. Assadi, M. Oghabi, D. Herlach, Influence of ordering kinetics on dendritic growth morphology, Acta Materialia, 57 (2009) 1639-1647.

[12] W. Boettinger, M. Aziz, Theory for the trapping of disorder and solute in intermetallic phases by rapid solidification, Acta Metallurgica, 37 (1989) 3379-3391.

[13] R. Ahmad, R. Cochrane, A. Mullis, Disorder trapping during the solidification of βNi3Ge from its deeply undercooled melt, Journal of Materials Science, 47 (2012) 2411-2420.

[14] K. Biswas, G. Phanikumar, D. Holland-Moritz, D.M. Herlach, K. Chattopadhyay, Disorder trapping and grain refinement during solidification of undercooled Fe–18 at% Ge melts, Philosophical Magazine, 87 (2007) 3817-3837.

[15] D.M. Herlach, Metastable materials solidified from undercooled melts, Journal of Physics: Condensed Matter, 13 (2001) 7737.

[16] A. Nash, P. Nash, Binary Alloy Phase Diagrams, in: US National Bureau of Standards Monograph Series 25, Elsevier, ASM, Ohio, 1976, pp. 35.

[17] S. Jin, C. Leinenbach, J. Wang, L.I. Duarte, S. Delsante, G. Borzone, A. Scott, A. Watson, Thermodynamic study and re-assessment of the Ge-Ni system, Calphad, 38 (2012) 23-34.

[18] Y. Ma, A.J. Ardell, The Nickel-Rich Region of the Ni-Ge Phase Diagram, Journal of phase equilibria and diffusion, 33 (2012) 4-8.

[19] O. Oloyede, T.D. Bigg, R.F. Cochrane, A.M. Mullis, Microstructure evolution and mechanical properties of drop-tube processed, rapidly solidified grey cast iron, Materials Science and Engineering: A, 654 (2016) 143-150.

[20] R. Ahmad, R. Cochrane, A. Mullis, Disorder trapping during the solidification of β-Ni$_3$Ge from its deeply undercooled melt, Journal of Materials Science, 47 (2012) 2411-2420.

[21] N. Haque, R.F. Cochrane, A.M. Mullis, Rapid solidification morphologies in Ni 3 Ge: Spherulites, dendrites and dense-branched fractal structures, Intermetallics, 76 (2016) 70-77.

[22] A. Mullis, D. Walker, S. Battersby, R. Cochrane, Deformation of dendrites by fluid flow during rapid solidification, Materials Science and Engineering, A304-306 (2001) 245-249.

<u>Highlights</u>

- A dendritic to seaweed growth transition is identified in rapidly solidified Ni3Ge.
- Confirmation of seaweed transition in congruently melting, cubic intermetallics.
- Transition appears to be mediated by change to non-cubic crystallography.